FED-Vol. 185, Numerical Methods in Multiphase Flows
ASME 1994

ON THE NUMERICAL TREATMENT OF INTERPHASE FORCES IN TWO-PHASE FLOW

Paulo J. Oliveira
Departamento de Electromecânica
Universidade da Beira Interior
Covilhã, Portugal

Raad I. Issa
Department of Mechanical Engineering
Imperial College of Science, Technology and Medicine
London, United Kingdom

ABSTRACT

In Eulerian computations of two-phase flow, iterative methods are usually employed to solve the discretised sets of equations (comprised of the momentum and continuity equations for each phase) that govern the flow. The iterative process is often troublesome in its convergence behaviour and sometimes fails to converge at all. A major role in affecting the robustness and stability characteristics of the solution algorithm is known to be played by the magnitude of the interphase force term in the momentum equations and by how it is treated numerically.

In this paper different schemes for treating the interphase force term in an iterative procedure based on the pressure-correction principle are examined; they range from the fully explicit (where the whole of the term is evaluated at the previous iteration) to an almost fully implicit treatment based on the elimination of phase velocities from the momentum equations of the counterpart phase.

The schemes are applied to the computation of dispersed bubbly flow in one- and two-dimensional configurations for a wide range of loading (i.e. average phase fraction) and of bubble diameter. The performance of the schemes is compared against each other. It is shown that in some cases only the fully implicit treatment is able to produce converged results.

1. INTRODUCTION

One of the two basic approaches to the mathematical modelling of two-phase flows is the Eulerean two-fluid model (Ishii 1975), where both phases are treated as inter-penetrating continua whose motion is governed by appropriately averaged conservation equations written for each phase. After averaging, interphase terms arise in the momentum equations, representing forces due to transfer of momentum and mass between the phases, such as drag, virtual mass etc., and these terms must be modelled. When the partial differential equations comprising these forces are solved numerically, by means of iterative finite-difference or finite-volume methodology, convergence problems may arise due to the magnitude of the interphase force term (Stewart & Wendroff 1974). It is the purpose of the present paper to analyse different ways of handling this term numerically.

In general the interphase force ($\vec{\mathbf{F}}_D$) may be linearised by writing it as proportional to the relative velocity ($\mathbf{u}_r$); thus, for example for the liquid phase in a dispersed gas (G) – liquid (L) mixture:

$$\vec{\mathbf{F}}_{D_L} = F_D(\mathbf{u}_G - \mathbf{u}_L),$$

where the parameter F_D is in general a function of the volume fraction ($\alpha \equiv \alpha_G$), the physical properties of the continuous phase (the liquid) and also, in most cases, of the relative velocity itself. In the case when the interphase force is due to drag only:

$$F_D = C_f \cdot g(Re_b) \cdot f(\alpha),$$

The drag factor C_f is defined as $C_f \equiv 18\mu_L/d_b^2$ (μ: viscosity; d_b: bubble diameter) and g is a function of the bubble Reynolds number ($Re_b=\rho_L d_b u_r/\mu_L$), given for example by $g=1+0.15Re_b^{0.687}$ as in Wallis (1969). $f(\alpha)$ is a function of the volume-fraction α which can be used as a corrective factor for high concentrations; the symmetric equation $f(\alpha)=\alpha(1-\alpha)$ is adopted here as the base $f(\alpha)$-function since it tends to the right limits whenever α tends to 0 or to 1. For low α, $f(\alpha)$ becomes equal to α, as it should for monodispersed spheres. For low Re_b the function g is approximately 1, and the drag is linearly related to the relative velocity $u_r \equiv \| \mathbf{u}_G - \mathbf{u}_L \|$. For high Re_b the drag becomes non-linear in u_r.

It is also useful to define a time scale for the drag interaction as:

$$\tau_{D_L} = \rho_L d_b^2/18\mu_L,$$

which is called the relaxation time (in this case for the liquid) and is related to the drag factor via $C_f=\rho_L/\tau_{DL}$. Note that the relaxation time associated with the gas phase is smaller than τ_{DL} by a factor $\rho_L/\rho_G \simeq 10^3$ for an air–water mixture.

The problems associated with the numerical implementation of the drag force occur because the relaxation time (especially for the gas) is usually small compared with the time-step δt used in the computations, and this implies that $\vec{F}_D$ should be treated implicitly. As an illustration, for air–water flow with 1 mm bubbles $\tau_{DL} = 1000 \times (10^{-3})^2/18/10^{-3} = 0.055$ s, $\tau_{DG} \sim 10^{-5}$ s, and $C_f=1.8\ 10^4$. The value of the drag is given by the product of a large number (C_f) by a small number ($u_r \simeq 0.1$ m/s). As a consequence any error in u_r, which is likely to occur during the iterative procedure, would be magnified by a factor equal to C_f, and this lies at the root of the convergence problems.

There are a number of ways to treat the drag term numerically and this is the subject of this paper. In section 2, the equations to be solved are given and the numerical method is described. This is followed by a description of the different algorithms used to deal with the drag term (section 3), and the results of application of these algorithms is given in section 4. From a comparison of the algorithm performance, conclusions about suitability of each method can be drawn (section 5).

2. EQUATIONS

In this section the governing equations are stated and the solution procedure is explained. This will be restricted to the necessary details, since most of it is well-established; the method is based on the finite-volume approach with its extension to non-staggered meshes (see Peric, 1985).

2.1 Differential Equations

The two-fluid model equations, restricted to incompressible flow without phase change, can be written in terms of phase-averaged velocity and pressure as:

$$\rho_k\left(\frac{\partial}{\partial t}\alpha_k + \nabla\cdot\alpha_k\tilde{\mathbf{u}}_k\right) = 0, \tag{1}$$

$$\rho_k\left(\frac{\partial}{\partial t}\alpha_k\tilde{\mathbf{u}}_k + \nabla\cdot\alpha_k\tilde{\mathbf{u}}_k\tilde{\mathbf{u}}_k\right) = -\alpha_k\nabla\tilde{p} + \nabla\cdot\alpha_k\boldsymbol{\tau}_k^t + \rho_k\alpha_k\tilde{\mathbf{g}} + \mathbf{F}_{D_k}. \tag{2}$$

In the equations of continuity (1) and momentum (2), the index k denotes the phases (c for the continuous phase and d for the dispersed one); it has also been assumed that the same pressure acts on both phases and that interfacial-averaged values of pressure and viscous stress equal the corresponding bulk phase values. The turbulent stress is given by a Newtonian-like expression:

$$\tau_k^t = \mu_k^t(\nabla\tilde{\mathbf{u}}_k + \nabla\tilde{\mathbf{u}}_k^T) - \tfrac{2}{3}(\mu_k^t\nabla\cdot\tilde{\mathbf{u}}_k + \rho_k k_k)\boldsymbol{\delta}, \tag{3}$$

where the eddy viscosities (μ^t) are obtained from a turbulence model, similar to what is used in single-phase modelling. Since the objective of the present paper is the numerical formulation of the interphase force term, details pertaining to turbulence modelling are excluded (this is given in Oliveira 1992).

2.2 Discretised Equations

The above differential equations are discretised by integration over hexahedral cells forming the computational mesh. A non-staggered type of mesh is used, whereby all main variables are stored at cell centres. In what follows the nomenclature illustrated in Fig. 1 is adopted. Locations where variables, or differences of variables (e.g. Δp), are computed are denoted with superscripts (either "P" for the cell centre, or "f" for the face along direction $l=f$). Following standard methods for non-staggered meshes (e.g. Peric 1985) all the resulting algebraic equations may be cast in the general linearised form:

$$A_P\phi_P = \sum_{f=1}^{6} A_f\phi_f + S^\phi, \tag{4}$$

where S is the source term and the A's are coefficients obtained from the discretisation of the convection and diffusion terms in the diferrential equations. When the upwind scheme is used, the expression for A is:

$$\begin{aligned} A_f &= D_f + \mathrm{Max}(F_f,0) \quad \text{for } f=f^-, \\ &= D_f - \mathrm{Min}(F_f,0) \quad \text{for } f=f^+, \end{aligned} \tag{5}$$

with the diffusion flux defined by

$$D_f = (\frac{\alpha\mu}{\mathcal{V}})^f \sum_j^3 B_{fj}^f B_{fj}^f = \frac{\overline{(\alpha\mu)}^f}{\mathcal{V}_f} B_f^2 , \tag{6}$$

and the convective flux defined by:

$$F_f = \widetilde{\alpha}^f \rho \sum_j B_{fj}^f \widetilde{u}_j^f . \tag{7}$$

In these equations, the overbar denotes arithmetic average, B_{li} is the i-component of the area-vector orientated along l-direction, B_f is the face area, $\mathcal{V}$ is the cell volume, $\mathcal{V}_f$ is calculated as $\mathcal{V}_f \equiv \sum_j [\Delta x_j]_f^f B_{fj}^f$, and $\widetilde{\alpha}^f$ is an upwinded volume-fraction at point "f" obtained from either α_P or α_F (Fig. 1) according to the sign of $F'_f \equiv \sum_j B_{fj}^f \widetilde{u}_j^f$. The cell "face-velocities" $\widetilde{u}$ are interpolated at cell faces using a special interpolation practice so that pressure decoupling on the non-staggered mesh is avoided. The actual expression used for the face fluxes is somewhat involved and can be found in Oliveira (1992). Hereafter the contribution of surrounding cells will be denoted as $H(\phi) \equiv \sum_f A_f \phi_f$, with $A_o \equiv \sum_f A_f$, and f=1 to 6 denote the faces. Also, all quantities are assumed to be located at cell-centre P, if a location index is not specified. The individual discretised momentum and continuity equations for each phase "k" are therefore:

$$\begin{aligned} (A_o^k + \frac{\alpha_k \rho_k \mathcal{V}}{\delta t}) u_{i_k} &= H_k^n(u_{i_k}) - \alpha_k^P \sum_l^3 B_{li}^P [\Delta p]_l^P \\ &+ F_D(u_{i_p} - u_{i_k})\mathcal{V} + S_{u_i}^k + \frac{\alpha_k \rho_k \mathcal{V}}{\delta t} u_{i_k}^n , \end{aligned} \tag{8}$$

$$\frac{\rho_k \mathcal{V}}{\delta t}(\alpha_k - \alpha_k^n) + \sum_f^6 (-1)^f F_{f_k} = 0 , \tag{9}$$

where the term $S_{u_i}^k$ contains all terms not explicitly written and index "p" denotes the other phase (i.e. $p \neq k$). The pressure correction equation will be based on the sum of dispersed and continuous phase continuities, hence from (9):

$$\begin{aligned} &\{\frac{\mathcal{V}}{\delta t}(\alpha_c - \alpha_c^n) + \sum_f^6 (-1)^f F_{f_c}/\rho_c\} \\ &+ \{\frac{\mathcal{V}}{\delta t}(\alpha_d - \alpha_d^n) + \sum_f^6 (-1)^f F_{f_d}/\rho_d\} = 0. \end{aligned}$$

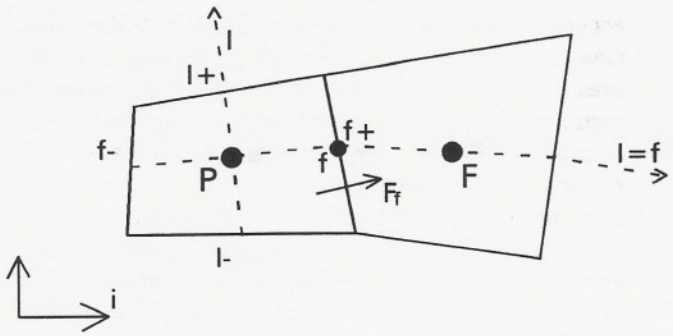

FIG. 1 GENERIC CELL (P) AND ITS NEIGHBOUR (F) ALONG DIRECTION f.

and since $\alpha_d + \alpha_c = \alpha_d^n + \alpha_c^n = 1$, the time derivative terms vanish leading to an overall continuity equation:

$$\sum_f^6 (-1)^f (F_{f_c}/\rho_c + F_{f_d}/\rho_d) = 0. \tag{10}$$

The equation used to compute α is based on the dispersed phase continuity; hence, starting from (9), with $k=d$, and after some re-arrangement the following transport equation for α is obtained:

$$\begin{aligned} (A_o^\alpha + \frac{\rho_d \mathcal{V}}{\delta t} + \mathrm{Max}[-\mathrm{div}(\mathbf{u}_d),0]\,)\,\alpha &= H_\alpha^n(\alpha) \\ &+ \mathrm{Max}[\mathrm{div}(\mathbf{u}_d),0]\,\alpha^n + \frac{\rho_d \mathcal{V}}{\delta t}\alpha^n, \end{aligned} \tag{11}$$

where the coefficients are now made up of convective fluxes only:

$$\begin{aligned} A_f^\alpha &= \mathrm{Max}(F'_{f_d},0) \quad \text{for } f=f^-, \\ A_f^\alpha &= -\mathrm{Min}(F'_{f_d},0) \quad \text{for } f=f^+. \end{aligned} \tag{12}$$

F' is a flux without volume-fraction (i.e. $F' \equiv F/\widetilde{\alpha}$) and $\mathrm{div}(\mathbf{u}_d) \equiv \sum_f^6 (-1)^f F'_{f_d}$.

3. SOLUTION ALGORITHM

3.1 The Base Solution Algorithm

The above sets of discretised equations are solved iteratively in a sequential manner whereby the velocity, pressure and scalars at a new time (or iteration) level ("$n+1$") are computed from their value at the previous time (or iteration) level ("n"). This advancement in time is used herein as a pseudo time-marching technique and may not be time

accurate. The algorithm falls in the fully-implicit class, with the pressure being obtained from a pressure-correction equation derived from a combination of the continuity and momentum equations. The explanation of the algorithm given below adopts the splitting concept and terminology introduced by Issa (1986). Here, for clarity, one of the formulations used to deal with the drag term is adopted; this will be called the base algorithm. The other interphase force formulations, which are described in the next sub-section, will not produce substantial alterations to the solution algorithm described here. The steps in the algorithm are:

1- Solve the continuous phase momentum equation (from (8) with k=c):

$$\left(\mathrm{A}_{\mathrm{O}}^{c}+\frac{\alpha_c\rho_c\mathcal{V}}{\delta t}\right)u_{i_c}^{*} = \mathrm{H}_{c}^{n}(u_{i_c}^{*}) - \alpha_c^{\mathrm{P}}\sum_{l}^{3}\mathrm{B}_{li}^{\mathrm{P}}[\Delta p^{n}]_{l}^{\mathrm{P}} + \mathrm{F}_{\mathrm{D}}(u_{i_d}^{n}-u_{i_c}^{n})\mathcal{V} + \mathrm{S}_{u_i}^{c}+\frac{\alpha_c\rho_c\mathcal{V}}{\delta t}u_{i_c}^{n}, \quad (13)$$

where "$*$" denotes intermediate values. Analogy with Eq. (4) yields: $\mathrm{A}_{\mathrm{P}}^{u_c} \equiv \mathrm{A}_{\mathrm{O}}^{c}+(\alpha_c\rho_c\mathcal{V})/\delta t$.

2- Solve the dispersed phase momentum equation (from (8) with k=d):

$$\left(\mathrm{A}_{\mathrm{O}}^{d}+\frac{\alpha\rho_d\mathcal{V}}{\delta t}+\mathrm{F}_{\mathrm{D}}\mathcal{V}\right)u_{i_d}^{*} = \mathrm{H}_{d}^{n}(u_{i_d}^{*}) - \alpha^{\mathrm{P}}\sum_{l}^{3}\mathrm{B}_{li}^{\mathrm{P}}[\Delta p^{n}]_{l}^{\mathrm{P}} + \mathrm{F}_{\mathrm{D}}\mathcal{V}u_{i_c}^{*} + \mathrm{S}_{u_i}^{d}+\frac{\alpha\rho_d\mathcal{V}}{\delta t}u_{i_d}^{n}, \quad (14)$$

with $\mathrm{A}_{\mathrm{P}}^{u_d} \equiv \mathrm{A}_{\mathrm{O}}^{d}+(\alpha\rho_d\mathcal{V})/\delta t+\mathrm{F}_{\mathrm{D}}\mathcal{V}$. Notice that the drag term in (13) is treated explicitly, whereas it is implicitly incorporated in Eq. (14). This practice is analysed in the next sub-section.

3- Assemble the pressure correction (p') equation based on the overall continuity (10). The pressure and velocities are updated according to the equations formulated by Issa & Oliveira (1993). These are:

$$\mathrm{A}_{\mathrm{P}}^{p}p_{\mathrm{P}}' = \sum_{f}\mathrm{A}_{f}^{p}p_{f}' + \mathrm{S}_{u}^{p}, \quad (15)$$

$$\left(\frac{\alpha_c\rho_c\mathcal{V}}{\delta t}\right)(u_{i_c}^{n+1} - u_{i_c}^{*}) = -\alpha_c^{\mathrm{P}}\sum_{l}^{3}\mathrm{B}_{i}^{\mathrm{P}}[\Delta p']_{l}^{\mathrm{P}}, \quad (16)$$

$$\left(\frac{\alpha_d\rho_d\mathcal{V}}{\delta t}+\mathrm{F}_{\mathrm{D}}\mathcal{V}\right)(u_{i_d}^{n+1} - u_{i_d}^{*}) = -\alpha_d^{\mathrm{P}}\sum_{l}^{3}\mathrm{B}_{i}^{\mathrm{P}}[\Delta p']_{l}^{\mathrm{P}}, \quad (17)$$

$$p^{n+1} = p^{n} + p'. \quad (18)$$

The fluxes F^{*} are corrected in the same way as the nodal velocities (Eqs. (16) and (17)) and the corresponding expressions are (see Issa & Oliveira 1993):

$$\mathrm{F}_{f_d}^{n+1} = \mathrm{F}_{f_d}^{*} - \mathrm{A}_{f_d}^{p}[\Delta p']_{f}^{f}, \quad (19)$$

$$\mathrm{F}_{f_c}^{n+1} = \mathrm{F}_{f_c}^{*} - \mathrm{A}_{f_c}^{p}[\Delta p']_{f}^{f}. \quad (20)$$

The pressure-correction coefficients appearing in Eqs. (15) – (20) are given by:

$$\mathrm{A}_{f}^{p} = \left(\frac{\widetilde{\alpha_c}\overline{\alpha_c}}{\overline{\mathrm{A}_{c}'}}+\frac{\widetilde{\alpha}_d\overline{\alpha_d}}{\overline{\mathrm{A}_{d}'}}\right)\mathrm{B}_{f}^{2} \equiv \mathrm{A}_{f_c}^{p}+\mathrm{A}_{f_d}^{p}, \quad (21)$$

$$\mathrm{A}_{\mathrm{P}}^{p} = \sum_{f}\mathrm{A}_{f}^{p}, \quad (22)$$

$$\mathrm{S}_{u}^{p} = -\sum_{f}^{6}(-1)^{f}\,(\mathrm{F}_{f_c}^{*}/\rho_c + \mathrm{F}_{f_d}^{*}/\rho_d). \quad (23)$$

In Eq. (21) the velocity coefficients A_{k}' are defined as $\mathrm{A}_{k}' = \mathrm{A}_{\mathrm{P}}^{u_k} - \mathrm{A}_{\mathrm{O}}^{k}$, being therefore (from (13) and (14)):

$$\mathrm{A}_{c}' = \frac{\alpha_c\rho_c\mathcal{V}}{\delta t}, \qquad \mathrm{A}_{d}' = \frac{\alpha_d\rho_d\mathcal{V}}{\delta t} + \mathrm{F}_{\mathrm{D}}\mathcal{V}. \quad (24)$$

4- Solve for all additional scalar equations. In the present case these are the turbulence quantities to be solved for, k and ϵ. With new values of k and ϵ the liquid and gas effective viscosities are updated.

5- The dispersed phase continuity equation (11) is solved implicitly in order to obtain an updated void-fraction ($\alpha \equiv \alpha_d$):

$$\left(\mathrm{A}_{\mathrm{O}}^{\alpha}+\frac{\rho_d\mathcal{V}}{\delta t}+\mathrm{Max}[-\mathrm{div}(\mathbf{u}_d),0]\right)\alpha^{*} = \mathrm{H}_{\alpha}^{n}(\alpha^{*}) + \mathrm{Max}[\mathrm{div}(\mathbf{u}_d),0]\,\alpha^{n} + \frac{\rho_d\mathcal{V}}{\delta t}\alpha^{n}. \quad (25)$$

The updated void-fraction and gas flux directions are used to determine upwinded cell-face void-fractions, $\widetilde{\alpha}^{f}$, which are stored.

With this the algorithm for two-phase flow computations is complete. The solution will be advanced in time until the normalised residuals of all the equations are smaller than a specified value (we use 10^{-4}). At this point the solution is said to be converged and, since overall continuity for the sum of gas and liquid is satisfied together with that of the gas, continuity will also be satisfied for the liquid phase.

3.2 Algorithm Variants

To clarify subsequent explanation, the discretised

equations of motion of the two phases (1 for continuous and 2 for dispersed) are re-written in a concise manner as (from Eq. (8)):

$$A_1 u_1 = F_D(u_2-u_1)\mathcal{V} + B_1$$
$$A_2 u_2 = F_D(u_1-u_2)\mathcal{V} + B_2, \qquad (26)$$

where the B,s contain all terms on the rhs of Eq. (8) except interphase force. The different algorithms dealing with this force are outlined in what follows.

1- Base algorithm. Here the force is incorporated explicitly in the continuous phase momentum equation and implicitly in the dispersed phase equation, as outlined in section 3.1:

$$A_1 u_1 = F_D(u_2^n-u_1^n)\mathcal{V} + B_1,$$
$$(A_2+F_D\mathcal{V})u_2 = F_D\mathcal{V}\, u_1^n + B_2. \qquad (27)$$

(The superscript "n" denotes previous time-level.)

2- Variant 2. The drag term is treated implicitly in both momentum equations, thus:

$$(A_1+F_D\mathcal{V})u_1 = F_D\mathcal{V}\, u_2^n + B_1,$$
$$(A_2+F_D\mathcal{V})u_2 = F_D\mathcal{V}\, u_1^n + B_2. \qquad (28)$$

3- Variant 3. Equations (26) are pre-arranged algebraically so that the second-phase velocity is eliminated from the first-phase momentum equation, and vice-versa. Starting from:

$$(A_1+F_D\mathcal{V})u_1 = F_D\mathcal{V}u_2 + B_1,$$
$$(A_2+F_D\mathcal{V})u_2 = F_D\mathcal{V}u_1 + B_2,$$

eliminate u_2 from the first equation to obtain:

$$(A_1+FAC_2\cdot A_2)u_1 = B_1 + FAC_2\cdot B_2,$$
$$(A_2+FAC_1\cdot A_1)u_2 = B_2 + FAC_1\cdot B_1, \qquad (29)$$

where FAC_1 and FAC_2 are generally denoted by FAC_i which is given by:

$$FAC_i = (F_D\mathcal{V}) \,/\, (A_i+F_D\mathcal{V}), \qquad (30)$$

and A_i denotes either A_1 or A_2.

4- Variant 4. In the equation for each phase, the velocity of the second phase is linearised about its previous time-level value; an algebraic pre-elimination, as in variant 3, is then applied. The derivation for phase-1 is as follows. The velocity u_2 present in the drag term is linearised as:

$$u_2 = u_2^n + \delta u_2,$$

so that the phase-1 equation becomes:

$$A_1 u_1 = F_D\mathcal{V}(u_2^n+\delta u_2-u_1) + B_1.$$

The increment δu_2 is obtained from an approximate momentum equation for phase-2, where the interphase force is the only retained term:

$$\delta u_2 = F_D\mathcal{V}\,\delta u_1 \,/\, (A_2+F_D\mathcal{V}) =$$
$$= F_D\mathcal{V}(u_1-u_1^n) \,/\, (A_2+F_D\mathcal{V}).$$

The equation for phase-1 becomes, after replacing δu_2 from expression above:

$$A_1u_1=F_D\mathcal{V}\Big(u_2^n+F_D\mathcal{V}(u_1-u_1^n)/(A_2+F_D\mathcal{V})-u_1\Big)+B_1,$$

or,

$$\Big(A_1 + F_D\mathcal{V} - \frac{(F_D\mathcal{V})^2}{A_2+F_D\mathcal{V}}\Big)u_1 =$$
$$= B_1 + F_D\mathcal{V}\,(u_2^n - \frac{F_D\mathcal{V}}{A_2+F_D\mathcal{V}}u_1^n\,).$$

This expression can be written in a form similar to the previous variant by making use of FAC defined above,

$$(A_1+FAC_2.A_2)\,u_1 = B_1$$
$$+\ FAC_2\,(\,A_2u_2^n + F_D\mathcal{V}(u_2^n-u_1^n)\,), \qquad (31)$$

and similarly for the second phase:

$$(A_2+FAC_1.A_1)\,u_2 = B_2$$
$$+\ FAC_1\,(\,A_1u_1^n + F_D\mathcal{V}(u_1^n-u_2^n)\,).$$

The pressure-correction equation is derived from the momentum equations and must therefore be modified for each of the variants mentioned. The way to do this follows closely the derivation of the pressure equation outlined in section 2.1, the modifications being self-evident except perhaps for variant 3. That derivation is based on a splitting

procedure where the only retained terms are the pressure gradient and the inertia term (here denoted $E \equiv \alpha\rho\mathcal{V}/\delta t$); as a consequence, the diagonal coefficients of the u equations in variant 3 (i.e. $A_i+FAC_j.A_j$ in Eq. (29)), will appear in the denominator of the pressure coefficients, with the A,s replaced by E,s (cf. Eqs. (13) and (14) against Eqs. (16) and (17)). Hence the coefficients of the pressure correction equation in variant 3, instead of being given by Eq. (21), are given by:

$$(A_f^p)_1 = (\overline{\alpha}_1\widetilde{\alpha}_1)^f \; B_f^2 \left(E_1+\frac{F_D\mathcal{V}E_2}{E_2+F_D\mathcal{V}}\right)^{-1}$$

$$(A_f^p)_2 = (\overline{\alpha}_2\widetilde{\alpha}_2)^f \; B_f^2 \left(E_2+\frac{F_D\mathcal{V}E_1}{E_1+F_D\mathcal{V}}\right)^{-1} . \qquad (32)$$

In these expressions f denotes face values, and α_i is the volume fraction of phase i, which can be the arithmetic average value ($\overline{\alpha}$) or the upwinded value ($\widetilde{\alpha}$) at the face.

3.3 Remarks

The simplest and perhaps most common algorithm to treat the interphase force is variant 2, where the force is implicitly incorporated in both phase momentum equations (see Stewart & Wendroff 1984). Looney *et al.* (1985) argue that this treatment leads to slow convergence when F_D is large and show that variant 1 when implemented in conjuction with the PISO method of Issa (1986) improves the convergence rate. The authors pointed out that improvement can be expected mainly if the volume fraction of the dispersed phase remains small over the whole region of interest as was the case with their solid-liquid calculations. Otherwise the dispersed phase may become a continuous one (say if $\alpha>0.5$) and the implicit/explicit treatment accorded to the phase equations would have to be interchanged. For these authors, such a problem did not arise because they were dealing with solid–liquid flow at low solid-fraction. The resulting equations in variant 4 show some similarities with those of the full elimination (compare (29) and (31)), but some degree of approximation is brought in. The advantage of this variant is that less computer storage is required than with variant 3. As for the full elimination, it was first used in conjunction with the two-fluid model by Harlow & Amsden (1975) and extended later by Spalding (1980). The form given above is slightly different from the one used by Spalding with the attendant differences in the formulation of the pressure-correction equation.

4. RESULTS

Two sets of cases were used to test the different algorithm variants. In the first a simple one-dimensional bubbly flow in a vertical channel was devised. The purpose of this case was to eliminate the algorithms that are fundamentally flawed; if the method does not work well in a simple 1-D situation it would be very unlikely that it could cope with complex multi-dimensional flow.

The second case was a more realistic one in which a complex flow pattern is obtained and where phase segregation and flow recirculation occur. The case chosen was the two-dimensional bubbly flow through a T-junction.

For both of the above test cases, calculations were performed over a wide range of realistic values of C_f the drag factor defined in section 1. It should be stressed, however, that the results of this study are not restricted to the drag force as all interphase forces can be accorded the same treatment. It is only because drag is usually the dominant force that it is singled out for treatment here.

One-Dimensional Tests

Details of the case are:
Fluid densities: ρ_1=1000 Kg/m^3; ρ_2=1 Kg/m^3.
Pipe dimensions: diameter D=50 mm, length L=500 mm.
Inlet conditions: $u_1=u_2=U$ = 1.0 m/s; α_2=0.10 .
Initial conditions: zero field for all dependent variables (α,u_1,u_2,p).
Time-step δt=0.1 s., corresponding to a local Courant number ($u\delta t/\delta x$) of 2.
The linear drag is given by $F_D=C_f\alpha(1-\alpha)$, that is $f(\alpha)=\alpha(1-\alpha)$.

The results of calculations for several drag coefficients C_f (non-dimensional $\overline{C}_f \equiv C_fU/\Delta\rho g$, varying from 10^{-2} to 10^5) are shown in Fig. 2 where the number of iterations to convergence is plotted against C_f. It is seen that the only method able to cope with very high C_f is variant 3, i.e. the full elimination. For this method the number of time-steps to convergence (N_t) remains fixed at 43 while $\overline{C}_f$ varies from 10^2 to infinity. All the other methods fail for large C_f, variant 2 being the more robust with convergence for $C_f=10^3$ but requiring a smaller time step of 0.01 sec. The first variant to fail

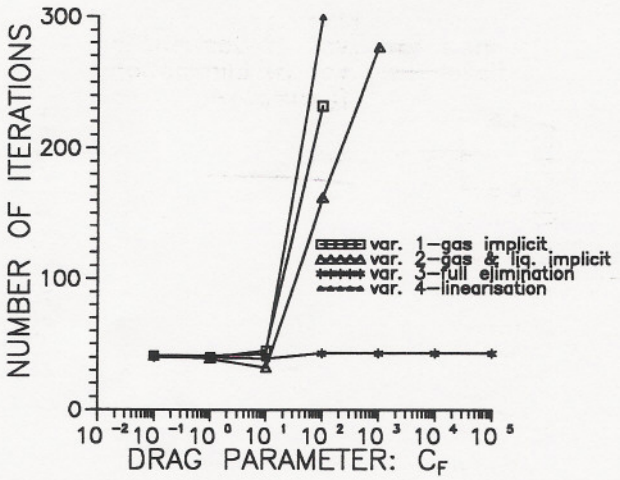

FIG. 2 NUMBER OF ITERATIONS TO CONVERGE DIFFERENT DRAG FORMULATIONS (LINEAR DRAG).

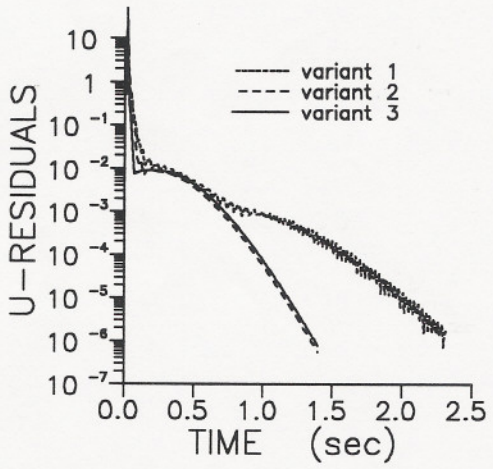

FIG. 4 RESIDUAL HISTORY FOR THREE DRAG FORMULATIONS ($\overline{C}_f = 10^2$; $\delta t = 0.01$ s).

is no. 4, the linearisation procedure, and this may be explained by the presence in Eq. (31) of terms $F_D(u_1^n - u_2^n)$, which adversely affects stability whenever F_D is large.

Further illustration of the aforementioned trends is provided by Figs. 3 and 4 which present the decay of u_1-residuals as a function of time (which can be seen as an iteration counter). Figs. 3 (a) and 3 (b) show the residual history for variant 2 and 3, respectively, for $\overline{C}_f = 10^1, 10^2, 10^3$ and 10^4 with $\delta t = 0.1$ sec. The full elimination (variant 3) shows identical behaviour for all values of C_f, whereas for the

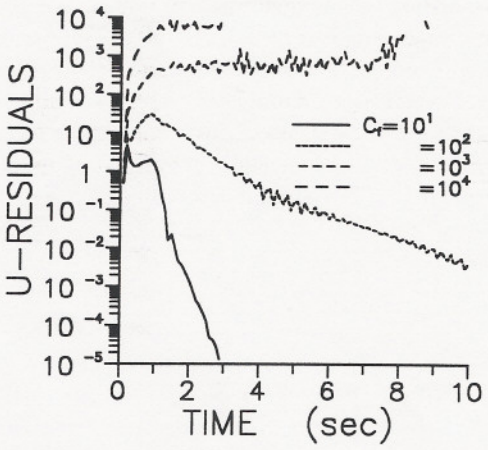

a) Variant 2: implicit drag in both gas and liq. equations.

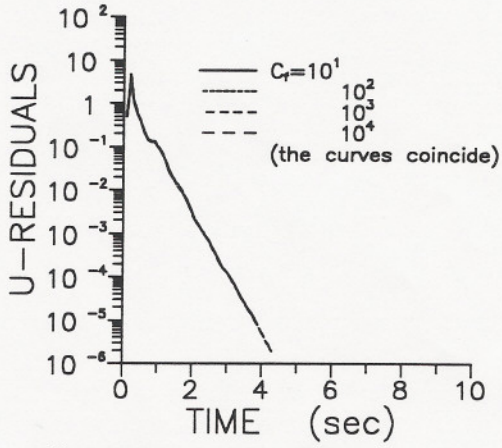

b) Variant 3: full elimination

FIG. 3 RESIDUAL HISTORY FOR 4 DRAG FACTORS ($\overline{C}_f = 10^1, 10^2, 10^3, 10^4$).

standard implicit treatment (variant 2) convergence is not obtained for $\overline{C}_f$ greater than 10^3. Figure 4 compares the residual decay for variants 1,2 and 3, at $\overline{C}_f = 10^2$ and with a time step smaller than before, $\delta t = 0.01$ sec. Here it can be seen that variant 1, although eventually converges, is on the verge of instability.

Two-Dimensional Tests

The previous results revealed the good stabilising effect of full elimination (variant 3). This is now tested in more complex situations, where recirculation may be present, and strong phase

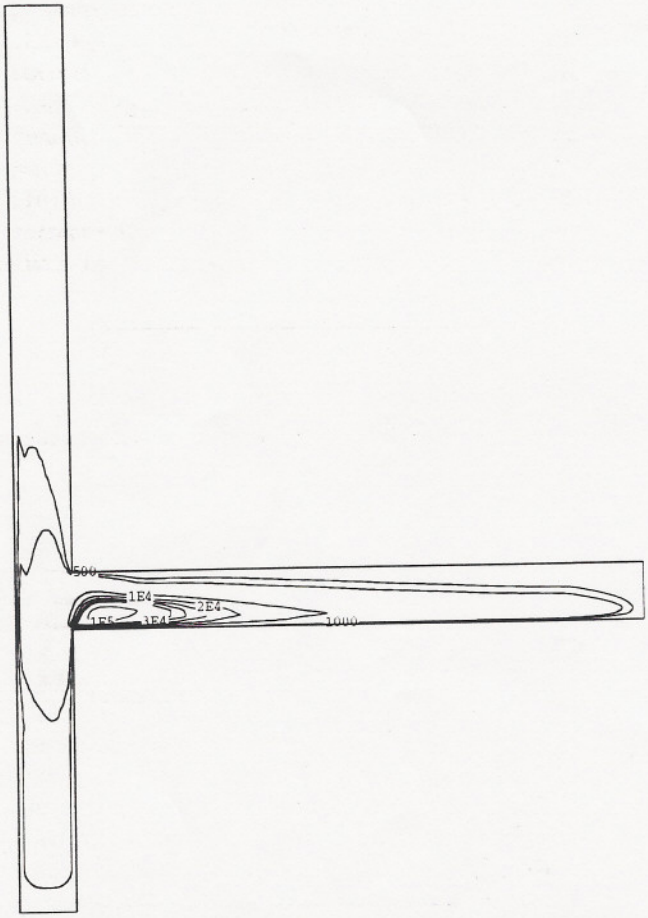

FIG. 5 CONTOURS OF THE DRAG PARAMETER F_D (Kg/sm^3) FOR BUBBLY FLOW IN A T-JUNCTION.

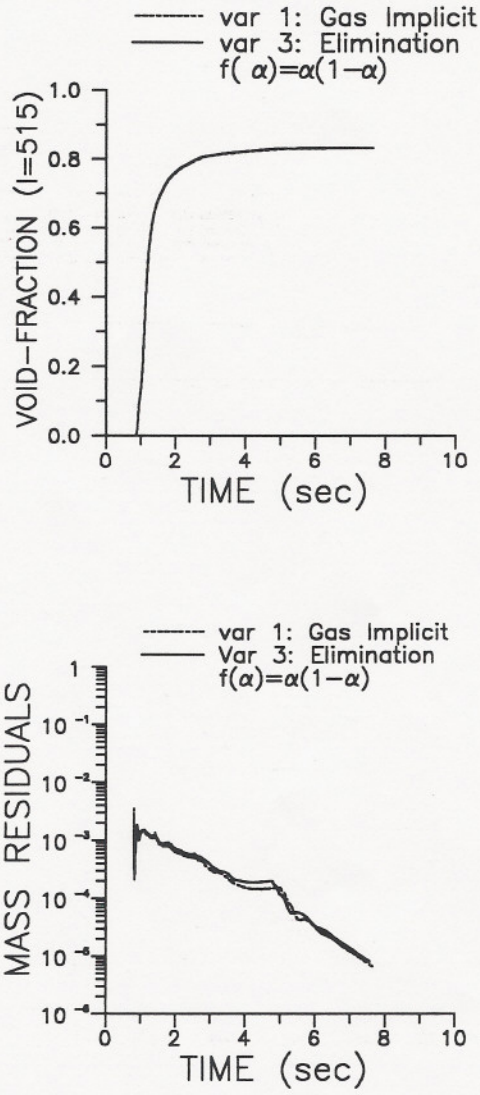

FIG. 6 COMPARISON OF TWO DRAG FORMULATIONS USING A TWO-PHASE FLOW IN A T-JUNCTION, WITH $f(\alpha)=\alpha(1-\alpha)$.

segregation occurs; the case chosen is that of bubbly flow in a two-dimensional T-junction (Issa & Oliveira 1990). The improved linearisation algorithm (variant 4) has also been tested but showed little difference compared with variant 1 (base method); hence it is not discussed further. Variant 2 was rejected because of its poor initial performance, showing little improvement over the base method, and is therefore excluded from the tests.

In this test-run the simulation is that of a low-quality bubbly air – water mixture, flowing along a straight main-branch and, at the T-junction, part of the flow is diverted into a side-branch forming an angle at 90 degrees with the main-branch. The area-averaged inlet conditions were: phase velocities, $u_G = 1.60$ m/s and $u_L = 1.53$ m/s; void-fraction, $\alpha = 2.08$ %. The bubble diameter was assumed to be 1 mm. For the cases considered here the overall extraction ratio at the junction was fixed at $Q_3/Q_1 = 0.38$, where Q is the volumetric flow-rate, subscript 1 is inlet arm and 3 is side-branch arm. In the recirculation zone (located at the side-branch of the Tee) there are high local void-fractions. Figure 5 shows contours of the drag parameter F_D (kg/sm^3) for this flow, with $f(\alpha) = \alpha/(1-\alpha)^2$. These contours serve to illustrate the non-uniformity of the drag-force field and the flow pattern. It is known that the concentration of air bubbles follows approximately the same contour-shape (Issa & Oliveira, 1990), with

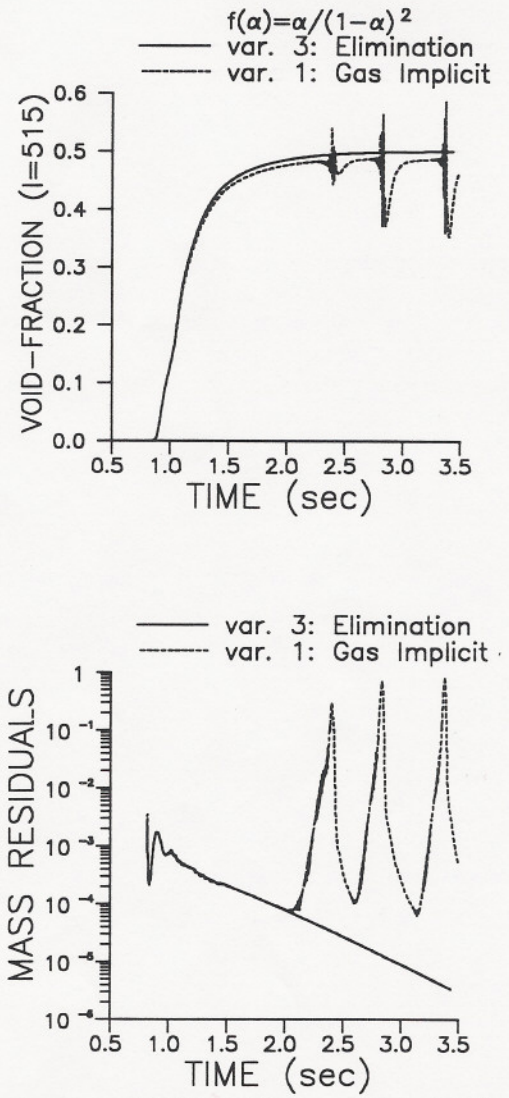

FIG. 7 COMPARISON OF TWO DRAG FORMULATIONS USING A TWO-PHASE FLOW IN A T-JUNCTION, WITH $f(\alpha)=\alpha/(1-\alpha)^2$.

a peak of α around 70 % at the point where F_D is maximum (Fig. 5), compared with 2 % at inlet.

Figure 6 presents the history of mass residuals and void-fraction at a given cell for variants 1 and 3, for the case when $f(\alpha)$ introduced in section 1 is taken as $\alpha(1-\alpha)$. In this particular case, both algorithms perform equally well and converge smoothly.

Figure 7 depicts the residual history for another case in which the drag force is divided by $(1-\alpha)^3$ to account for bubble/bubble interaction as suggested by Zuber (1964). Thus $f(\alpha)$ defined in section 1 becomes equal to $\alpha/(1-\alpha)^2$. As a consequence when α is large and non uniform, the interphase force varies considerably across the domain; in this case 500 fold variations were obtained in the magnitude of the force (cf. Fig. 5). Such variations become a source of instability which the elimination algorithm in variant 3 is able to cope with; on the other hand the base method fails to converge as can be seen in Fig. 7.

5. CONCLUSIONS

A study of the numerical treatment of the interphase force embodied in the multidimensional two-fluid model equations has been carried out, using a finite-volume method and a pressure correction technique. From tests, it is shown that special treatment of the interphase drag term in the numerical solution algorithm is sometimes crucial for obtaining convergence of the iteration process. Several variants for the drag term treatment are analysed and tested. From the evidence presented it may be concluded that:

i) When the interphase force is either large or highly non-uniform, only the full elimination method (variant 3) could converge.

ii) When the force is not large or non-uniform, both variants 1 and 3 behave similarly.

iii) The additional cost for implementing variant 3 is 3 arrays of memory in 2-D (4 arrays in 3-D). However, this is a small price to pay to ensure robustness of the numerical scheme and at times it is the only alternative that would succeed in obtaining a solution.

REFERENCES

Harlow, F.H., and Amsden, A.A., 1975, "Numerical calculation of multiphase fluid flow," *J. Comp. Phy.*, Vol. 17, pp. 19-52.

Ishii, M., 1975, *Thermo-Fluid Dynamic Theory of Two-Phase Flow*, Eyrolles, Paris.

Issa, R.I., 1986, "Solution of the implicitly discretised fluid flow equations by operator-splitting," *J. Comp. Phy.*, Vol. 62, 40-65. (also Rep. FS/82/15, Mec. Eng. Dep., Imperial College, London, 1982).

Issa, R.I., and Oliveira, P.J., 1990, "A multidimensional approach to the prediction of two-phase flow in T-junctions," *Int. Conf. of Basic Principles and Industrial Applications of Multiphase Flow*, IBC, London.

Issa, R.I., and Oliveira, P.J., 1993, "Numerical

prediction of phase separation in two-phase flow through T-junctions," *Computers and Fluids*, Vol. 23, No. 2.

Looney, M.K., Issa, R.I, Gosman, A.D., and Politis, S., 1985, "A two-phase flow numerical algorithm and its application to solid/liquid suspension flows," Imperial College Rep. FS/85/31.

Oliveira, P.J., 1992, "Computer modelling of multidimensional multiphase flow and application to T-junctions," Ph.D. Thesis, Imperial College, Univ. of London.

Peric, M., 1985, "A finite volume method for the prediction of three-dimensional fluid flow in complex geometries," Ph.D. Thesis, Imperial College, Univ. of London.

Spalding, D.B., 1980, "Numerical computations of multiphase flow and heat transfer," *Recent Advances in Numerical Methods in Fluids,* Vol. 1, Ed. C. Taylor and K. Morgan, Pineridge Press.

Stewart, H.B., and Wendroff, B., 1984, "Two-phase flow: models and methods," *J. Comp. Phy.*, Vol. 56, pp. 363-409.

Wallis, G.B., 1969, *One Dimensional Two-Phase Flow*, McGraw-Hill, New York.

Zuber, N., 1964, "On the dispersed two-phase flow in the laminar flow regime," *Chemical Engng. Sci*, Vol. 19, pp. 897-917.